

Square Pulse Galvanostatic Synthesis and Characterization of Nano- Copper Oxide

Hassan Karami^{1,2,*}, Boshra Afshari²

¹Department of Chemistry, Payame Noor University, 19395-4697, Tehran, I.R. of Iran

²Nano Research Laboratory, Department of Chemistry, Payame Noor University, Abhar, Iran

*E-mail: karami_h@yahoo.com

Received: 27 June 2016/ Accepted: 28 August 2016 / Published: 30 December 2016

In this study, the copper oxide nanoparticles are synthesized by the square pulse galvanostatic method (SPGM) through anodic oxidation of copper electrode in sodium sulfate solution. The released Cu²⁺ ions are precipitated slowly as Cu(OH)₂ nanoparticles. In the temperature more than 40 °C, the copper hydroxide is decomposed to CuO nanoparticles. The electrochemical cell includes one copper positive electrode (anode) and two copper negative electrodes (cathodes) in the sodium sulfate solution as electrolyte. The effects of some parameters such as solution temperature, electrolyte concentration, pulse time, relaxation time and pulse amplitude were studied and optimized. The optimum conditions for the electrosynthesis of copper oxide nanoparticles includes 1×10⁻⁴ M sodium sulfate solution, the square pulse amplitude of 20 mA cm⁻², pulse time of 2 s, relaxation time of 1 s and temperature of 60°C. The produced samples are filtered and washed 3 times with water and finally with acetone and then dried at 600°C for 1 h. The prepared samples are characterized by SEM, TEM and XRD techniques. The experimental data show the optimized copper oxide sample includes uniform CuOnanorods with 35 nm average diameter and 550 nm average length.

Keywords: Square pulse, galvanostatic, electrosynthesis, copper oxide, nanorods.

1. INTRODUCTION

In recent years, there is a lot of interest about the semiconductor nano- crystals because of their properties such as increased chemical activity, a large surface area, electronic and optical properties as compared to those of the bulk materials [1,2]. The transition semiconductors have wide applications in various fields such as solar energy transformation, magnetic storage media, catalysis and electronics [3–12]. Copper oxide as a transition metal oxides has shown particular chemical reactivity due to their large surface areas and high dislocations [13]. CuO powder is a typical p type semiconductor with the narrow band gap of 1.2 eV and has promising applications in many fields such as in the active catalyst

[14,15], gas sensor [16-19], high efficiency thermal conducting material [20], magnetic recording media [21] and in solar cell applications [22].

Recently, some methods have been reported for the preparation of CuO nano-crystals such as co-implantation of metal and oxygen ions [23], thermal decomposition [24], the sonochemical technique[25], sol-gel method [26], chemical solid state reaction at room temperature [27], and electrochemical method [28].

In this study, the copper oxide nanorods were synthesized by the square pulse galvanostatic method (SPGM) through anodic oxidation of copper electrode in sodium sulfate solution. In this method, the effects of synthesis parameters such as pulse amplitude (pulse height), pulse time, relaxation time, electrolyte concentration and solution temperature. In this work, the effects of pulse time, relaxation time and solution temperature were investigated and optimized by the "one factor at a time" method.

2. EXPERIMENTAL

2.1. Materials

Sodium sulfate, glycerol, sodium dodecyl sulfate (SDS), Cetyltrimethyl ammonium bromide (CTAB), Triton x-114 and acetone were purchased from Merck. The pure copper sheets (purity > %99.5) were produced from Shaheed Bahonar copper Co. (Kerman, Iran). Double-distilled water was used in all experiments.

2.2. Instrumental

All the electrochemical experiments were carried out by means of a pulse electrolyzer (BTE 06 model), were made by Karami technical group (KTG) in Iran. The structures of synthesized samples were identified by Bruker XRD (D8 Adavance model) with copper K_{α} incident radiation. Philips XL-30 SEM and Zeiss CEM902A TEM were used to study the morphology and particle size of the samples. All SEM images were analyzed by Microstructure Measurement software to determine the average particle size. Size distribution was studied by dynamic light scattering (DLS) method ((Malvern, Zetasizer Nano ZS3600)).

2.3. Electrosynthesis procedure

Before any electrode position, the copper electrodes were put in the concentrated HNO_3 (65% w/w) for 30 s and then washed with double-distilled water to remove any surface oxidized impurities exposed to the air. Two copper cathodes were coupled with a copper anode, and immersed in sodium sulfate solution. The pulsed current were applied at different rates for the direct anodic oxidizing of copper electrode. The effects of the parameters such as pH, concentration of Na_2S , type and

concentration of the additive, the solution temperature, pulse time (t_{on}), relaxation time (t_{off}), and the pulsed current amplitude were optimized by the "one at a time" method.

3. RESULTS AND DISCUSSION

3.1. Pulse characterization

Copper oxide nanoparticles were directly prepared by the SPGM by using copper electrodes in sodium sulfate solution. Figure 1 shows the square pulse current (SPC) specification. As it can be seen in Fig. 1, the SPC has three variables, including pulse height (pulse amplitude), pulse time (t_{on}) and relaxation time (t_{off}). In the electrosynthesis application of SPC, the effects of SPC variables as well as synthesis physicochemical variables must be optimized. In the current study, the physicochemical variables include electrolyte concentration, solution temperature and the type and concentration of synthesis additive [29,30].

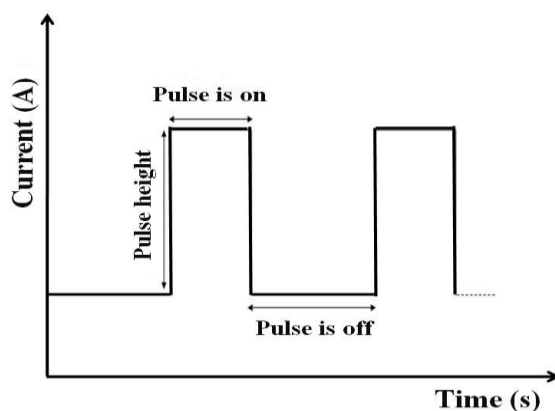


Figure 1. The SPC chart and its pulse variables.

3.2. Effect of synthesis temperature

Among the synthesis variables, the temperature of the solution had more influence on phase composition of the electrochemically prepared nanomaterials [31-34]. To investigate the effect of solution temperature on the morphology and the particle size of copper oxide, seven CuO samples were synthesized in various temperatures. In temperatures 20, 30 and 40 °C, the oxidation rate of copper and thus the precipitated yield is low. By increasing the temperature, the synthesis rate is increased.

When the synthesis is done in temperatures of 20, 30 and 40 °C, the color of yield is turquoise which is related to the formation of $\text{Cu}(\text{OH})_2$. The color of yield is dark in temperature above 50 °C which is related to the formation of CuO. On the other hand, with increasing temperature, the morphologies and the particles sizes of the CuO samples change (Fig. 2). When the electrosynthesis experiment was performed at temperature less than 60 °C, the reaction rate was very slow and the

synthesized nanoparticles were smaller than others but, not uniform. At temperatures higher than 60 °C, the reaction was fast, but the prepared samples also show non-uniform particles with more agglomeration. The results confirm that the copper oxide example, synthesized at 60°C has a homogeneous morphology and small particle size. The average particle size of the sample synthesized at 60 °C is 64 nm.

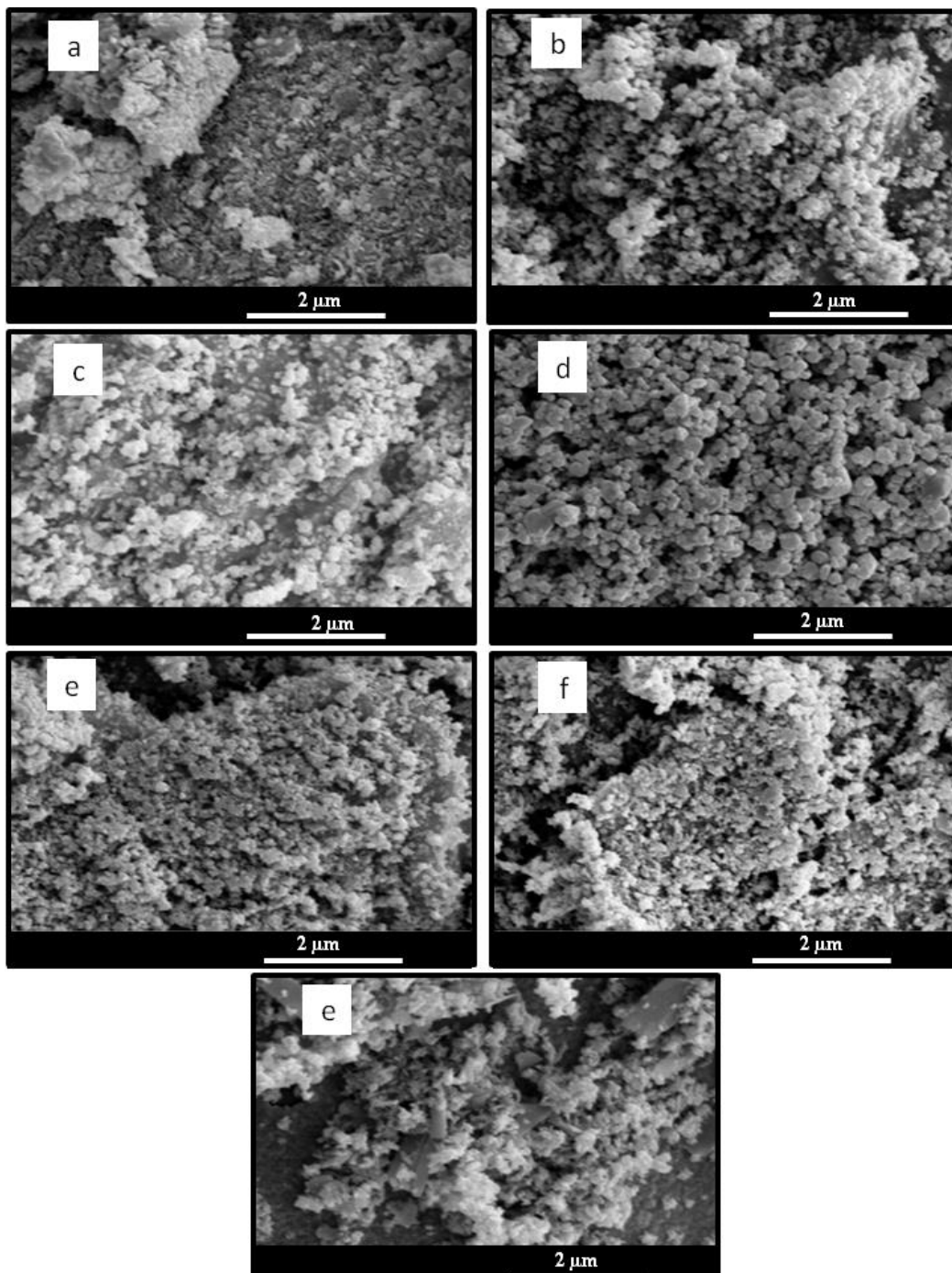


Figure 2. The SEM images of copper oxide samples which synthesized at temperatures 20 °C (a), 30 °C (b), 40 °C (c), 50 °C (d), 60 °C (e), 70 °C (f) and 80 °C (g); The other parameters were kept constant as sodium sulfide 0.01 M, $t_{off}=1$ s and $t_{on}=1$ s.

3.3. Effect of the current amplitude

In the chemical synthesis, the current amplitude is the main synthesis factor [29,30]. The effects of the height of the pulsed current was investigated on the morphology and the particle size of copper oxide samples. The amplitude of pulsed current varied from 5 to 77 mA cm⁻² while, the other parameters were kept constant (solution temperature of 60 °C, 0.01 M sodium sulfide, t_{off}= 1 s and t_{on}= 1 s). The synthesized copper oxide samples were characterized by SEM technique. Figure 3 shows the SEM images of the resultant copper oxide samples in various amplitudes of the current pulse.

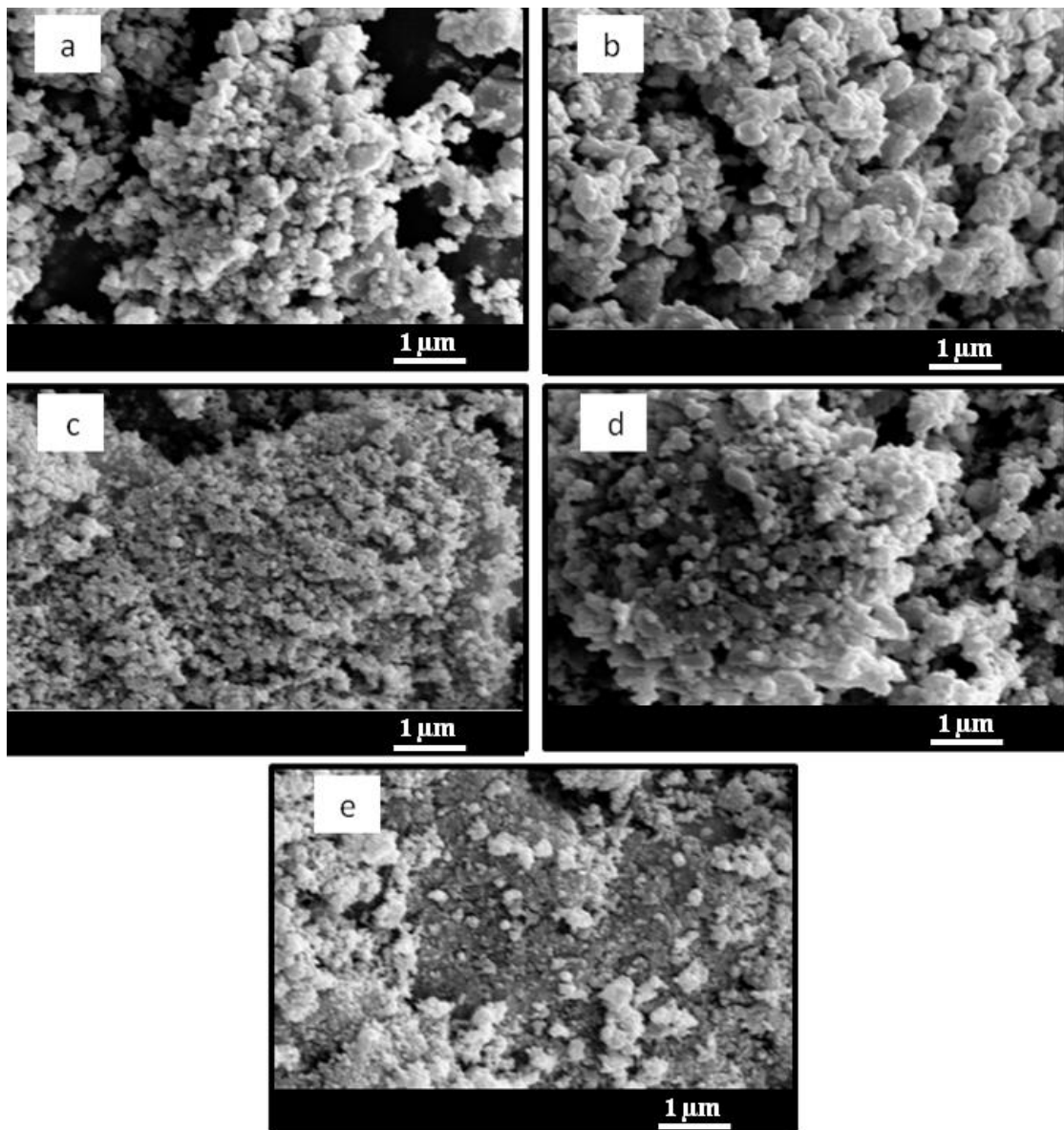


Figure 3. The SEM images of the synthesized copper oxide samples in various pulse amplitudes; 5 mA.cm⁻² (a), 10 mA.cm⁻² (b), 20 mA cm⁻² (c), 39 mA.cm⁻² (d) and 77 mA cm⁻² (e). The other experimental parameters were kept constant (solution temperature 60 °C, sodium sulfide 0.01 M, t_{off}=1 s and t_{on}=1 s).

It is obvious in Fig. 3 that the sample morphology as well as particles sizes strongly changes by variation in pulse height. Exerting of small current pulses causes to decrease the synthesis rate and form the big particles [32, 34]. In pulse height of 20 mA cm^{-2} , the sample consists uniform and small and nanoparticles. When the pulse heights above 20 mA cm^{-2} is used, the synthesis rate is increased. Nevertheless, the synthesized copper oxide particles not only are not uniform and homogeneous, but also are bigger than that's about 20 mA cm^{-2} .

3.4. The effect of t_{on}

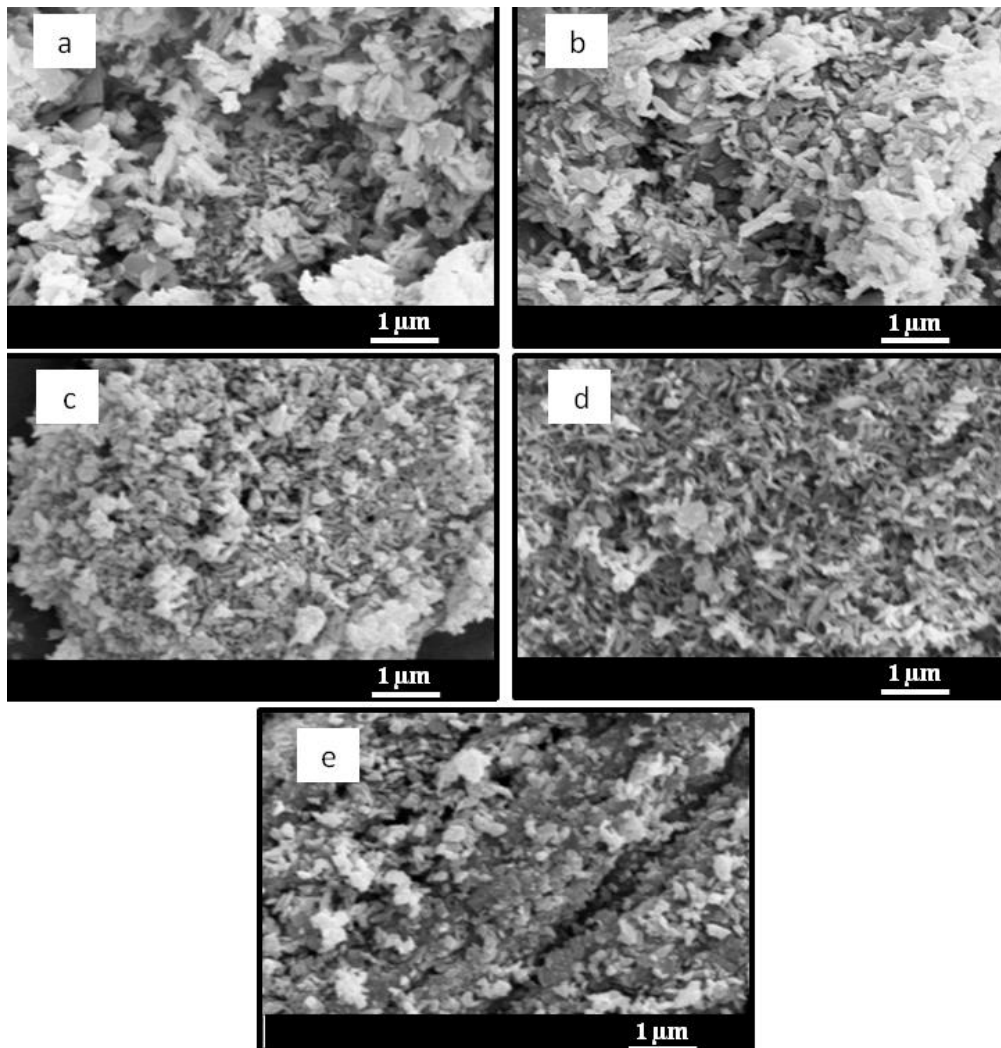


Figure 4. The SEM images of CuO samples synthesized in different pulse times; 0.25 (a), 0.5 (b), 1 (c), 2 (d) and 3 s (e). The other experimental parameters were kept constant as solution temperature 60°C , sodium sulfide 0.01 M and $t_{off}=1 \text{ s}$.

In this section, the effect of t_{on} was checked on the morphology and particle size of CuO samples. Each current pulse contains a controllable number of electrons that can change by variation of the pulse time [35]. In these experiments, the amounts of other parameters were kept constant (current density: 20 mA.cm^{-2} , sodium sulfide concentration: 0.01 M , temperature: 60°C and t_{off} : 1 s). Figure 4 shows the SEM images of CuO samples which synthesized at various pulse times. As it can be seen in

Fig. 4, at 0.25 s pulse time, the CuO particles were synthesized without any specific morphology. At the pulse time of 0.5 s, the particles become larger than those of 0.25 s without any uniform morphology but, the nanoplates begin to form. As Fig. 4c shows, the synthesized sample contains the small uniform nanoparticles somewhat. In the pulse time of 2 s, the particles size decrease and the morphology of particles are more uniform than previous samples. At the pulse time of 3 s, as it can be seen in Fig. 4f, the particles without uniform morphology are dispersed among the agglomerated particles. It can be resulted that the mechanism of synthesis is changed by increasing the pulse time and, more regular particles with better morphology are synthesized. However, with respect both particle size and morphology, pulse time of 2 s was selected as the optimal value.

The summary of SEM results of five different CuO samples which were synthesized at the different pulse times is shown in Table 1.

Table 1. The summary results of SEM studies of the five different CuO samples were synthesized in five different pulse times.

Sample	t _{on}	Average of length	Average of diameter	shape
a	0.25	380	87	Nanorod and
		87	40	Nanocrine
b	0.5	270	67	Nanorod
c	1	-	64	Spherical particle
d	2	213	56	Nanorod
e	3	157	70	Nanorod and
		-	127	spherical particle

3.5. The effect of t_{off}

The importance of this parameter was noted in some previous reports [29,30]. To study the relaxation time effect, six synthesis was performed at different levels of t_{off}. Figure 5 shows the SEM images of the synthesized CuO samples at various relaxation times. As it can be seen in Fig. 5, relaxation time as well as the previous variables can strongly change the CuO morphology. When exerting a current pulse into the cell, copper atoms are oxidized and copper oxide nanoparticles are formed. In relaxation time, the formed particles in the last current pulse can have a rearrangement in particle morphologies. Based on Fig. 6d, at the relaxation time of 2 s, CuO nanorods can be formed and selected as the best sample. The average particle size of all the samples was measured by the Microstructure software. The obtained results were summarized in Table 2. The results show when the relaxation time is increased, the morphology of CuO particles changes from spherical nanoparticles to nanorod particles as well as their sizes change.

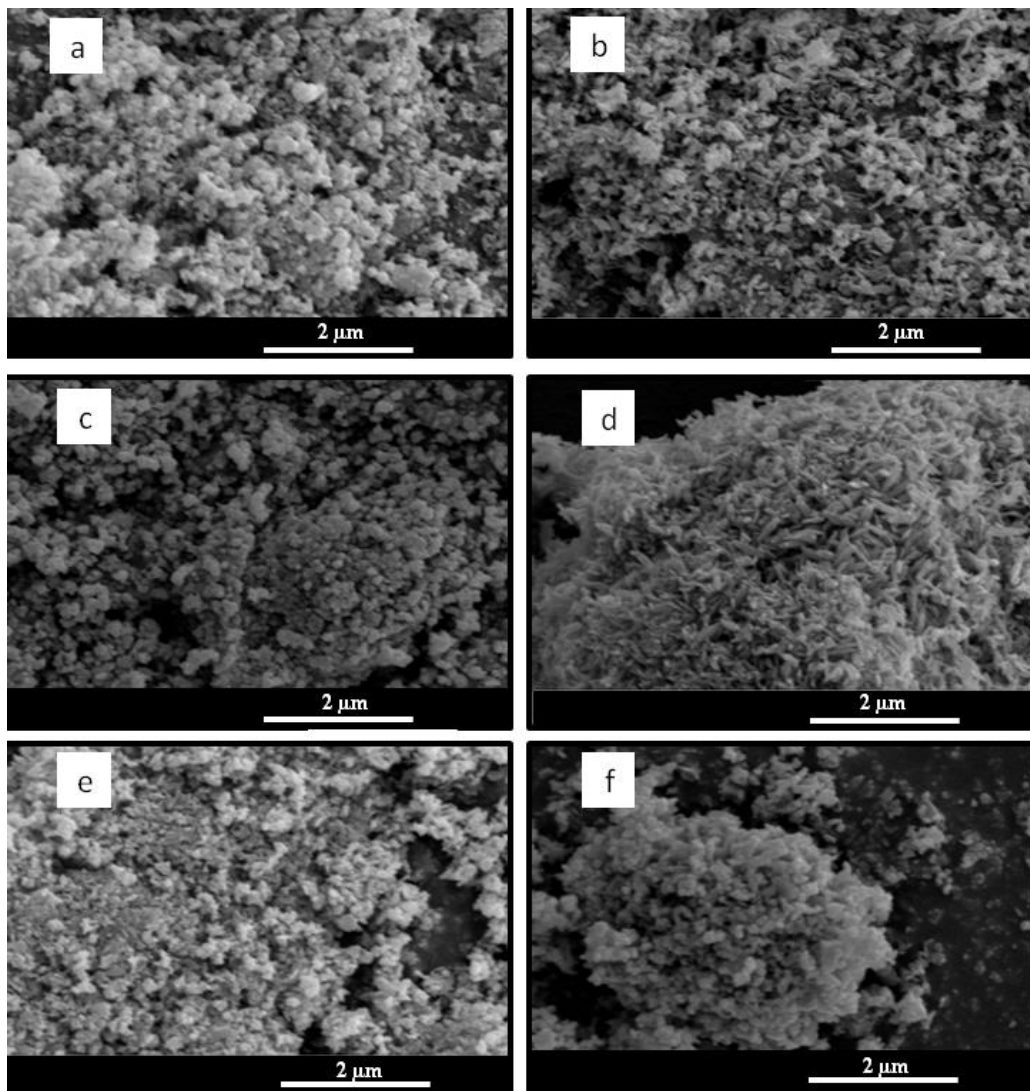


Figure 5. The SEM images of CuO samples synthesized in various relaxation times; 0 (a), 0.25 (b), 0.5 (c), 1 (d) 1.5 (e), and 2 s (f). The other parameters were kept constant as solution temperature 60 °C, sodium sulfide 0.01 M and $t_{on}=1$ s.

At relaxation time above 1 s, uniform nanorods is rearranged into spherical nanoparticles.

Table 2. The morphology and particle size of six different CuO samples were synthesized in different relaxation times.

sample	t_{off}	Average of length	Average of diameter	shape
a	0	-	72 485	Spherical clooney
b	0.25	163 -	72 52	Nanorod and Spherical
c	0.5	-	60 288	Spherical and clooney
d	1	205	56	Nanorod
e	1.5	190	25 72	Nanorod and Spherical
f	2	-	95	Spherical

3.6. Effect of sodium sulfate concentration

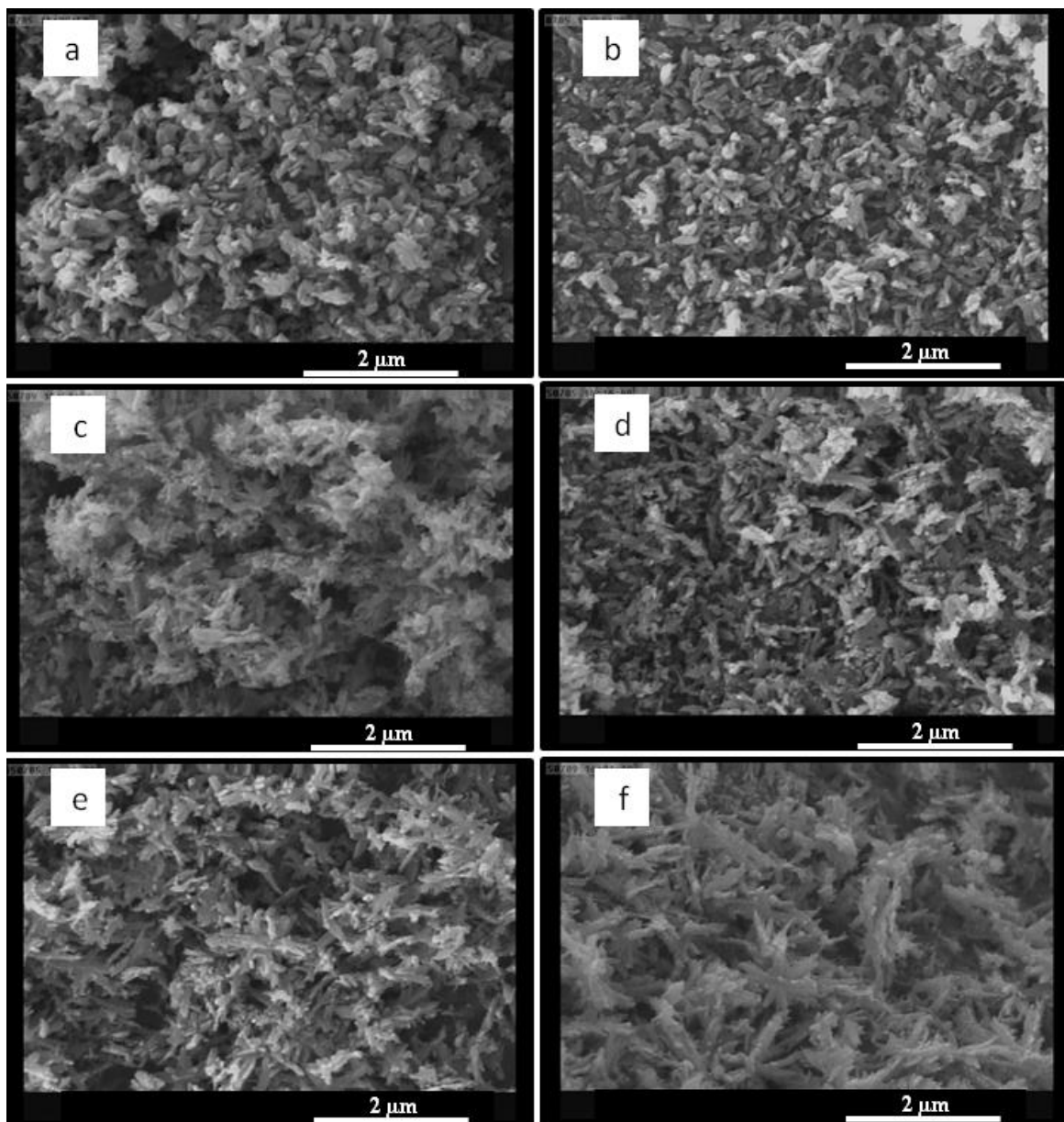


Figure 6. The SEM images of CuO samples which synthesized at sodium sulfide concentrations of 0.0001 M (a), 0.001 M (b), 0.005 M (c), 0.01 M (d), 0.1 M (e) and 0.5 M (f).

Table 3. Effect of electrolyte concentration on the morphology and particle size of CuO samples.

sample	Sodium sulfate(M)	Average length (nm)	Average diameter (nm)	Shape
a	0.0001	521	30	Nanorod
b	0.001	399	35	Nanodendrite
c	0.005	266	40	Nanodendrite and nanorod
d	0.01	482	45	Nanorod
e	0.1	214	75	Sub-microrod
f	0.5	268	110	Microrod

For the investigation of the effects of electrolyte concentration on the particle size and morphology of CuO samples, the amount of this parameter was changed from 0.0001 to 0.5 M while the other parameters were kept constant. The SEM images of CuO examples synthesized in various concentrations of sodium sulfide were shown in Fig. 6. In all previous samples, sodium sulfide concentration was 0.01 M. Based on the previous results, CuO nanorods can be synthesized in 0.01 M sodium sulfide solution (Fig. 5d and Fig. 6c). As Fig. 6 shows, electrolyte concentration has a strong effect on the sample morphology. In pure water (without sodium sulfide), the cell potential increases and the synthesis rate are negligible. In 0.0001 M sodium sulfide, synthesis rate is acceptable and the nanodendrites are formed. By increasing the electrolyte concentration from 0.0001 to 0.01 M (Figs. 6a, 6b, 6c and 6d), the CuO nanodendrites slowly converted to nanorods. At electrolyte concentration above than 0.01 M, the solution resistance and thus the cell potential are decreased during exerting current pulse. Therefore, CuO nanorods grow and become bigger (microrod in Fig. 6f). The average particles sizes of all samples of Fig. 6 were measured and the results were shown in Table 3.

For more characterization, the sample "d" in Table 3 was analyzed by TEM, DLS and XRD. Figure 7 shows two TEM images of copper oxide nanorods. Based on Fig. 7, the sample consists uniform CuO nanorod with 35 nm average diameter and 550 nm average length.

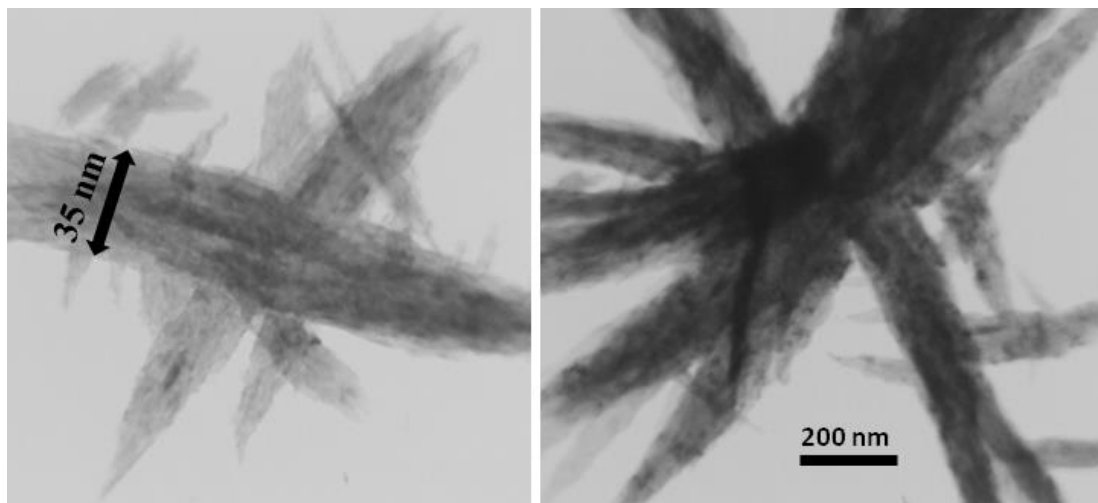
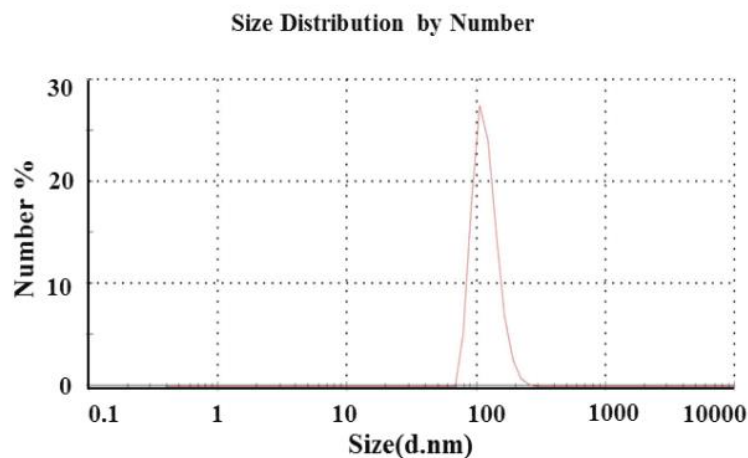
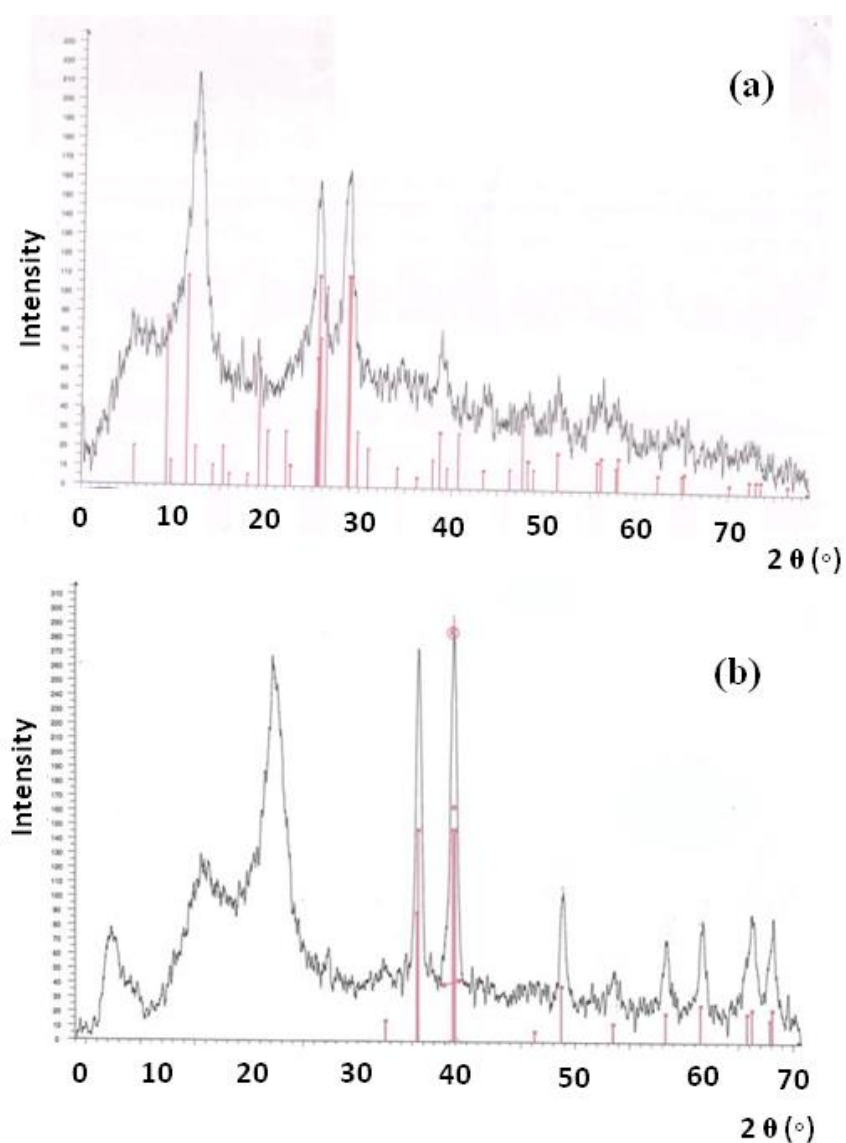


Figure 7. TEM micrographs of CuO sample synthesized in 20 mA.cm^{-2} current density, 0.01 M sodium sulfide, $t_{\text{on}} = 2 \text{ s}$, $t_{\text{off}} = 1 \text{ s}$, temperature of 60°C in the absence of any additive.

The sample was analyzed by DLS (Fig. 8). The DLS data shows that the particle size distribution is in the range of 70 to 250 nm with the average particle size of 105 nm. It should be mentioned that the dispersed light by the sample particles is measured in DLS method. Therefore, the dimensions of nanorods cannot be correctly measured by DLS. Any data in Fig. 8 is the number between the diameter and length of nanorods. For example, the average particle size in Fig. 8 is 105 nm which, this size is a number between 35 nm (average real diameter) and 550 nm (average real length).

**Figure 8.** DLS diagram of the CuO nanorods.**Figure 9.** The XRD pattern of the CuO sample synthesized at 70 °C; without annealing (a) and after annealing at 600 °C (b).

In XRD quantitative analysis, by comparing the integrated peaks of the known phases, their fraction can be identified. Based on this method, the phase structure and the composition of the CuO sample synthesized at 60 °C was twice characterized by XRD. In first time, the sample was synthesized at 60° C, filtered and dried at 70 °C for 24 h, and then, without any other thermal step was analyzed by XRD (Fig. 9a).

In second time, the dried sample was annealed at 600 °C (Fig. 9b). The results show that the sample without annealing step contains high amounts of impurity, but the annealed sample contains only pure copper oxide (CuO). In annealing process, all impurities are converted into CuO.

Based on the main peak in XRD patterns (Fig. 9b; $2\theta = 40$) and by the Debye- Scherrer equation, the average particle size was calculated 25 nm which confirmed by that's of TEM result.

3.7. The effect of synthesis additive

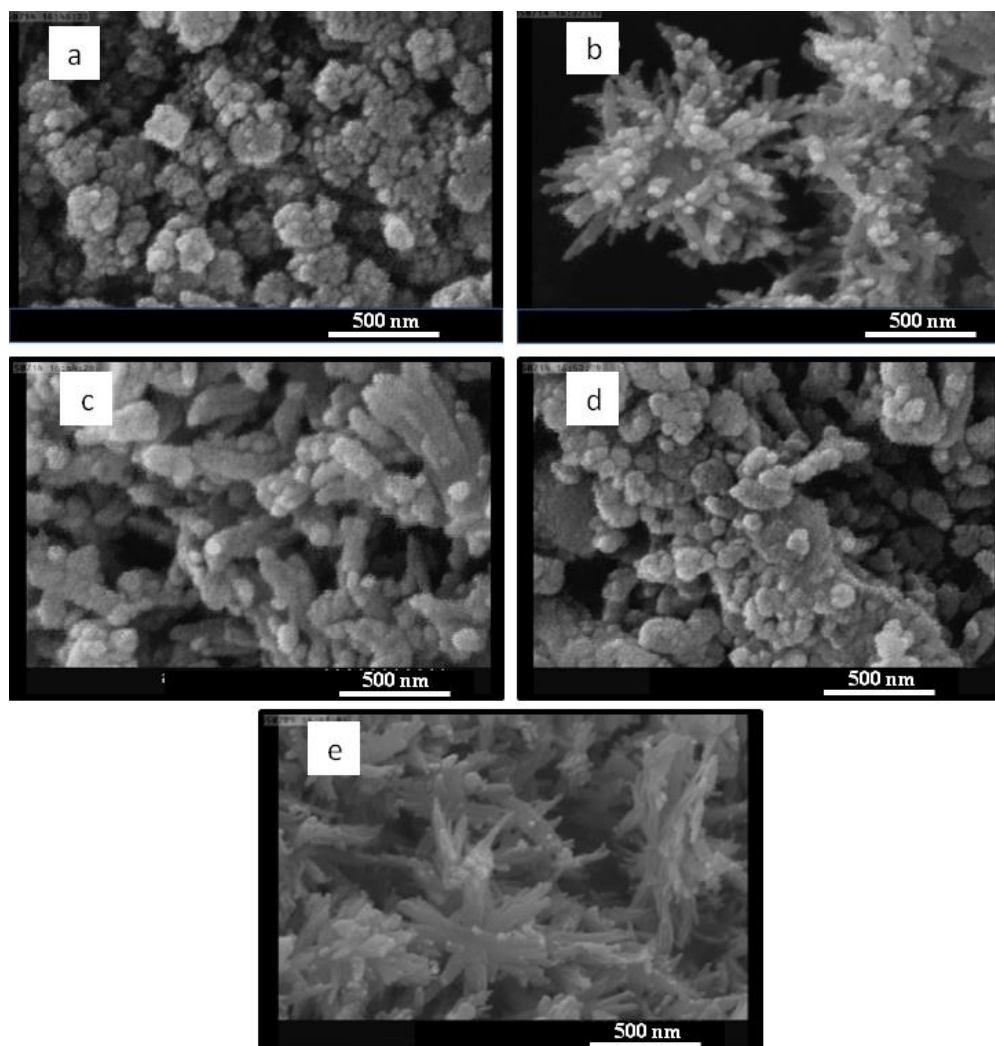


Figure 10. The SEM images of CuO samples synthesized in the presence of glycerol (a), SDS (b), CTAB (c), Triton X-114 (d) and without additive (e). The other synthesis parameters was kept constant as solution temperature 60 °C, sodium sulfide 0.01 M, $t_{off}=1$ s and $t_{on}=2$ s.

Our previous studies shows some compounds like sodium dodecyl sulfate (SDS), cetyltrimethyl ammonium bromide (CTAB), glycerol and Triton X-114 can be used as the manager of structure to achieve more uniform nanomaterials [36-38]. Therefore, the effects of all of the mentioned additives were investigated on the morphology and the particle sizes of CuO. In these experiments, all syntheses were done in sodium sulfate concentration of 0.0001 M. In Fig. 10, the SEM images of CuOsamplessynthesized in the presence of different additives were shown. As it can be seen in Fig. 10, in the absence of any additive, the CuOsampleconsistsnanodendrites (Fig. 10e). The presence of glycerol (Fig. 10a), SDS (Fig. 10b), CTAB (Fig. 10c) and Triton X-114 (Fig. 10d) in synthesis solution of CuO causes to form agglomerated spherical nanoparticles. Based on the previous reports [36-38], synthesis additives can change the nucleation and crystal growth rates. The obtained results showed that the presence of additive does not have a positive effect on the synthesized samples, thus, the CuOnanorodsshouldbesynthesizedwithoutany additive.

4. CONCLUSION

The presented results revealed that the square pulse galvanostatic method can be used as a confidence and effective technique for the synthesis of various copper oxide nanostructures by the direct anodic oxidation of the copper electrode in sodium sulfate. The times of pulse and relaxation steps, sodium sulfate concentration, the amplitude of pulsed current and synthesis temperature are the effective parameters can change the morphology and the particles sizes of the copper oxide samples. By changing synthesis conditions, snow can be synthesized in different morphologies such as nanoparticles, nanosheets, nanorods and etc.

ACKNOWLEDGEMENT

The authors would like to thank the financial support of this work by Abhar Payame Noor University Research Council.

References

1. A. Henglein, *Chem. Rev.* 89 (1989) 1861.
2. A. Agfeldt, M. Gratzel, *Chem. Rev.* 95 (1995) 49.
3. E.P. Wolfarth, Ferromagnetic Materials, Vol. II, NorthHolland, Amsterdam, New York, Oxford, Tokyo, (1980) P. 405.
4. J.C. Mallinson, The Foundations of Magnetic Recording, Academic Press, Berkeley, CA, (1987), Chapter 3.
5. F.N. Bradley, Materials for Magnetic Funtions, Hayden, New York, (1976), Chapter 2.
6. W. Oelerich, T. Klassen and R. Bormann, *J. Alloys. Compd.*, 315 (2001) 237.
7. O. Regan, M. Gratzel, *Nature* 353 (1991) 737.
8. K. Naazeeruddin, A. Kay, M. Gratzel, *J. Am. Chem. Soc.* 115 (1993) 6832.
9. U. Bjoerksten, J. Moser, M. Gratzel, *Chem. Mater.* 6 (1994) 858.
10. W.P. Dow, T.J. Huang, *J. Catal.* 160 (1996) 171.
11. P.O. Larsson, A. Andersson, R.L. Wallengerg, B. Svensson, *J. Catal.* 163 (1996) 279.
12. Y. Jiang, S. Decker, C. Mohs, K.J. Klabunde, *J. Catal.* 180 (1998) 24.
13. A.E. Rakhshni, *Solid State Electron.* 29 (1986) 7.

14. Y. Yecheskel, I. Dror, and B. Berkowitz, *Chemosphere*, 93 (2013) 172.
15. Q. Zhang, K. Zhang, D. Xu, G. Yang, H. Huang, F. Nie, C. Liu and S. Yang, *Prog. Mater. Sci.*, 60 (2014) 208.
16. P. Raksa, A. Gardchareon, T. Chairuangsri, P. Mangkorntong, N. Mangkorntong, S. Choopun, *Ceramics Int.*, 35 (2009) 649.
17. A. Aslani, V. Oroojpour, *Physica B: Cond. Mater.*, 406 (2011) 144.
18. M. Yang, J. He, X. Hu, C. Yan, Z. Cheng, *Environ. Sci. Tech.*, 45 (2011) 6088.
19. Y. Li, J. Liang, Z. Tao, J. Chen, *Mater. Res. Bull.* 43 (2008) 2380.
20. X. Wang, X. Xu, S.U.S Choi, J. *Thermophys. Heat Transfer* 13 (1999) 474.
21. S. Ishio, T. Narisawa, S. Takahashi, Y. Kamata, S. Shibata, T. Hasegawa, Z. Yan, X. Liu, H. Yamane, Y. Kondo and J. Ariake, *J. Magn. Magn. Mater.* 324 (2012) 295.
22. V. Kumar, S. Masudy-Panah, C. C. Tan, T. K. S. Wong, D. Z. Chi, G. K. Dalapati, Proceedings of the IEEE 5th International Nanoelectronics Conference (INEC '13) (2013) 443.
23. S. Nakao, M. Ikeyama, T. Mizota, P. Jin, M. Tazawa, Y. Miyagawa, S. Miyagawa, S. Wang, L. Wang, *Rep. Res. Cent. Ion Beam Technol., Hosei Univ. Suppl.* 18 (2000) 153.
24. J.Q. Yu, Z. Xu, D.Z. Jia, *Chin. J. Functional Mater. Instrum.* 5 (1999) 267.
25. R.V. Kumar, Y. Diamant, A. Gedanken, *Chem. Mater.* 12 (2000) 2301.
26. A.A. Eliseev, A.V. Lukashin, A.A. Vertegel, L.I. Heifets, A.I. Zhirov, Y.D. Tretyakov, *Mater. Res. Innovations* 3 (2000) 308.
27. J.F. Xu, W. Ji, Z.X. Shen, S.H. Tang, X.R. Ye, D.Z. Jia, X.Q. Xin, *J. Solid State Chem.* 147 (2000) 516.
28. K. Borgohain, J.B. Singh, M.V. Rama Rao, T. Shripathi, S. Mahamuni, *Phys. Rev.* 61 (2000) 11093.
29. H. Karami, A. Yaghoobi, A. Ramezani, *Int. J. Electrochem. Sci.*, 5 (2010) 1046.
30. H. Karami, M. Alipour, *Int. J. Electrochem. Sci.*, 4 (2009) 1511.
31. J. Park, J. Kim, H. Kwon, H. Song, *Adv. Mater.* 21 (2009) 803.
32. H. Karami, O. Rostami-ostadKalayeh, *J. Clus.Sci.*(2009).
33. E. Mazario, M. P. Morales, R. Galindo, P. Herrasti, N. Menendez, *J. Alloys Compd.*, 536, (2012) 222.
34. H. Karami, A. Kaboli, *Int. J. Electrochem. Sci.*, 5 (2010) 706.
35. G.p. Ocon, P. Herrasti, S. Rojas, *Polymer*. 42 (2001) 2439.
36. H. Karami, M. GhaleAsadi, M. Mansoori, *Electrochim. Acta*, 61 (2012) 154.
37. H. Karami, M.R. Hormozinezhad, S. Mohammadi, *Nanosci. Nanotech. Ind. J.*, 2 (2008) 70.
38. H. Karami, Z. Bigdeli, S. Matini, *Int. J. Electrochem. Sci.*, 11 (2016) 3095.